CHARACTERIZATION AND COMPARISON OF ACCELEROMETERS FOR LOW-FREQUENCY MODAL APPLICATIONS

Ron Merkel*, Michael J. Dillon*, Dr. David L. Brown°

*The Modal Shop, Inc.
1776 Mentor Ave. Suite 170
Cincinnati, Ohio 45212

°University of Cincinnati,
Structural Dynamics Research lab
Cincinnati, Ohio

ABSTRACT. *This paper overviews the selection process for transducers used for estimating experimental modal parameters below 0.5 Hz on aerospace and civil structures. Four different designs are examined, and their behavior is evaluated based on actual test data. A number of specifications are considered for review, including low frequency response behavior, resolution, and mass loading.*

1. Introduction

Transducer selection is an important facet of experimental modal analysis. A variety of technical specifications should be evaluated based upon the given applications. Since modal analysis is an applicable science for a multitude of structures ranging from large civil infrastructures to tiny computer disk drives, prudent examination of such transducer specifications as frequency response characteristics, sensitivity, resolution and sensor mass is critical to the experiment's success.

Typically, modal analysis sensor arrays are optimized for common modal test parameters in an effort to reduce the per channel cost of the system. This is important because large transducer channel counts are required for simultaneous acquisition, which eliminates roving and ensures uniform mass distribution to improve the consistency of the measurement database for a better modal model. Standard modal arrays are designed with the best compromise among frequency range, sensitivity, resolution and sensor mass. Thermal stability and durability are additional important practical considerations.

This paper focuses on very low frequency modal applications (less than 0.5 Hz), such as those found in the aerospace and civil infrastructure industries. For these cases, four accelerometers are presented as potential options. The focus on low frequency signals requires excellent signal resolution as well as thermal stability of the sensing element to prevent bias drift problems. Frequency response characteristics, both in magnitude and phase, are evaluated from 0.5 Hz down to 0 Hz. An important aspect to remember is that phase is a relative quantity among the array of sensors – if the entire array maintains consistent phase response characteristics, accurate results are ensured. Since a large number of transducers are used simultaneously, reasonable transducer mass is desirable to minimize mass loading effects on the modes of interest. However, sensor mass is relative to the test structure and should be evaluated as such.

Differences in these technical specifications are directly related to the type of sensing element used in the transducer design. Both piezoelectric and capacitive type transducers are compared here. Additionally, piezoelectric transducers can be either quartz or ceramic. An evaluation of these design considerations and ultimate transducer performance as applied to experimental modal analysis is quantified.

2. Transducer Design Overview

Three of the four transducers reviewed are piezoelectric, two of which use piezoceramic sensing elements, and one of which uses quartz. Both quartz and piezoceramic are popular choices for modal transducers, partly due to their use of convenient low impedance ICP® circuitry[1]. They have inherent differences, two of which are of particular interest to modal accelerometer evaluation. These include low frequency response function behavior and sensitivity to ambient temperature. The fourth transducer considered here is the variable capacitive type, which is capable of measurements to 0 Hz.

Low frequency response function magnitude is, of course, of primary interest when evaluating modal sensors. It is one of the more desirable properties of quartz. Quartz can be relied upon to give a flat response before being filtered by the electronics of the integrated amplifier. Piezoceramic, on the other hand, will have a rising electrical output for a given mechanical input when coupled to its charge amp. To counteract this, the time constant of the accelerometer is tuned such that the response magnitude is filtered back to within the required tolerance. The detrimental effect of the 1st order filtering is in the phase portion of the frequency response function. The shorter time constant causes the phase to shift higher in the frequency band of interest.

The temperature coefficient plots of otherwise similar accelerometers are shown in Fig. 1. The sensitivity shift of the quartz transducer is much lower than that of the ceramic sensor.

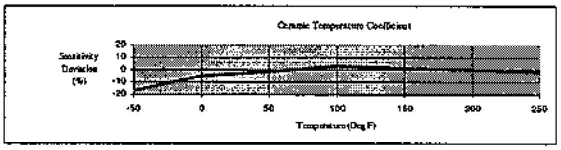

Fig. 1a. – Ceramic Temp. Coefficient

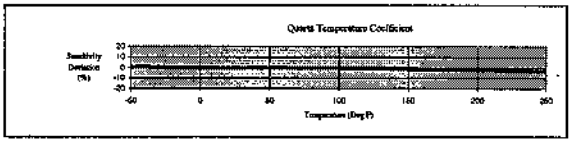

Fig. 1b. – Quartz Temp. Coefficient

The final accelerometer profiled here is of the variable capacitance type, capable of measuring at frequencies down to and including 0 Hz. It is unique in this regard due to the amplification circuits required by the other three. The common practice in piezoelectric transducers is to utilize FET based, impedance converting ICP® circuits which allow the measurement of signals over a reasonable cable length. The result is that the dynamic portion of the signal rides on a DC bias of usually 8 to 12 volts. The overall signal must be decoupled before going into an analog to digital converter.

This is not necessary in the 370A02's capacitive system, the output of which can be zeroed relative to gravity at the test site.

3. Transducer Characteristics

The sections below briefly describe the characteristics of each design, which are fully tabulated in Appendix A.

3.1. Quartz Shear-Mode Design – Characteristics

PCB's 353 Series of accelerometers have traditional piezoelectric quartz sensing element that is the most stable piezoelectric sensing material available. Due to the quartz design, this accelerometer has excellent low frequency phase characteristics. This design does have limited resolution due to the combination of quartz's relatively low piezoelectric output and the noise floor characteristics of the embedded voltage amplifier circuit.

3.2. Seismic Piezoceramic Shear – Characteristics

The 393 Series of accelerometers were designed primarily for seismic applications. These transducers are built around a ceramic piezoelectric element with an integrated charge amplifier. The ceramic element allows for flexible manufacturing of the element geometry which can result in lower manufacturing costs and unit pricing. The integrated charge amplifier provides higher resolution than its counterpart, the voltage amplifier (especially at lower frequencies). The ceramic element does exhibit higher thermal sensitivity than a quartz element and high thermal or mechanical shock can shift the sensitivity of the transducer.

3.3. High Gain Ceramic Shear – Characteristics

This accelerometer uses a ceramic element so it has general properties equivalent to those listed above for the 393 Series. The primary advantage of the 352M12 is that it has only 18% of the mass of the 393M52. It is also considerably smaller than the 393 and equal in size to the 353B52. The 352M12 has only one-fortieth the resolution of the 393 but twice the resolution of the 353B52 (Fig. 2).

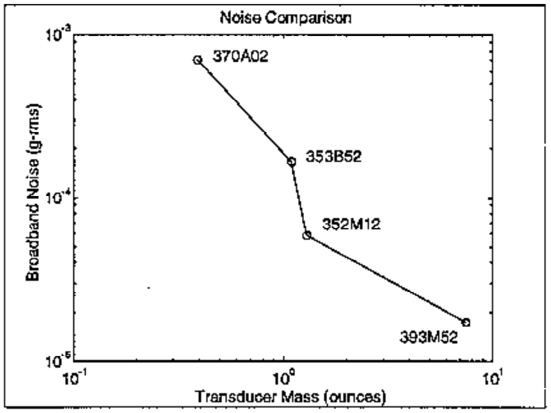

Fig. 2.

3.4. Capacitive DC Accelerometer – Characteristics

The 370A02 provides a true 0 Hz response with excellent resolution using a capacitive sensing element. The transducer has only one-third the mass of the 353B52 and the 352M12 and less than half the height. The 370 uses a 4 pin Microtech connector, and operates on a non-traditional 3 wire system.

4. Experimental Comparison

The noise floor of each accelerometer is compared in Fig. 3. Each transducer was mounted to a large mass that was placed on foam to isolate it from ground vibration. Data was then collected to provide the noise floor values at standard frequencies as well as the broadband level. The noise characteristics listed in Appendix A for each transducer are representative of actual testing conducted for this paper. As expected, the 393M52 has the lowest noise floor. The 352M12 and the 353B52 are comparable in weight but the noise floor of the ceramic 352M12 is significantly lower. A 3.5 Hz rocking resonance of the large mounting mass was excited by ambient ground vibration and can be seen in the traces of the 393 and the 352 (Fig. 3). The resonance does not appear in the traces of the 370 and 353 because their noise floors are equal to or greater than the level of the excitation during that particular measurement.

The phase shift between two accelerometers of each type is compared in Fig. 4. The frequency response function between each pair of accelerometers mounted to a long-stroke shaker was calculated. It is at this point that the *relative* phase characteristics of two accelerometers should be considered. Rather than the *absolute* phase, the relative phase could possibly be matched over a much broader frequency range than that of the absolute phase. The *relative* phase of the frequency response function for each pair is within one degree over the 0 to 25 Hz test span. This result shows that all of the accelerometers under consideration have stable and consistent phase characteristics. The absolute phase characteristics of each accelerometer type are included in Appendix A.

5. Beam Application

The dynamic response of a beam was measured with each of the accelerometers under consideration to show the effects of some of the important transducer characteristics. The accelerometers were placed adjacent to each other at the end of the beam throughout the testing. Power spectra were measured for a step release test. The results of this comparison are shown in Fig. 5. The first bending mode of the beam occurred at 1.0 Hz. As shown in Fig. 5, there are significant differences in the low-frequency response of the various accelerometers. The three accelerometers which were AC coupled show equivalent stiffness lines for the first bending mode and vary only in the location and noise floor of the anti-resonance. The DC coupled 370A02 shows a significantly different stiffness line and does not show an anti-resonance. The difference in stiffness line slope and the occurrence of an anti-resonance are the result of the AC coupling filter. These measurements were made on a HP35670 analyzer with an AC coupling filter that is specified to be <3 dB roll off at 1 Hz. This causes the accelerometer signal to roll-off significantly below 1 Hz. When AC coupling is applied to the 370A02, the results match those of the 393M52 showing that it is the AC coupling filter affecting the signals. This result is displayed in Fig. 6.

A more appropriate test using DC coupling was run to evaluate the low frequency measurement capability of the 370A02 capacitive accelerometers. Fig. 7 shows the response of both the 370A02 and a DC coupled 393M52. Their stiffness lines do not significantly deviate from each other until approximately 0.2 Hz. Note the significant deviation of the

AC coupled 393M52's stiffness line up near the resonance of the beam. It is this deviation that can cause miscalculation of several modal parameters including damping.

6. Conclusion

The information presented here shows the various design trade-offs that are possible when considering possible ultra-low frequency modal transducers. While each of these transducers are representative of what is possible from their given design, it should be remembered that for a given application, an accelerometer design can be tailored to fit appropriately.

Reiterating what was shown here, the use of a capacitive accelerometer is advantageous when absolute phase and magnitude characteristics are of utmost importance down to 0 Hz. Current drawbacks of this design are its broadband noise and non-traditional signal conditioning requirements. Although seldom selected for modal applications, quartz can still be considered if, for some reason, extreme mechanical or thermal transients are expected. These transients can permanently damage the sensing elements of the other options. Piezoelectric ceramic offers the highest resolution (lowest noise floor) for a given transducer mass (Fig. 2). Piezoceramic is the most desirable option when the testing environment is expected to be relatively stable, but can also encounter problems when considering absolute phase at very low frequencies.

Is there a simple answer to the question "What design offers the best modal transducer?" Probably not. But keeping the above things in mind when selecting a sensor will make you more educated when working with an applications engineer who can design one to fit your needs, or when trying to select the best "general purpose modal accelerometer" for your laboratory.

References:

1.) "General Signal Conditioning Guide to Piezoelectric ICP® and Charge Output Sensor Instrumentation", Document G-0001B, PCB Piezotronics, Depew, NY, 14043.

APPENDIX A:
ACCELEROMETER CHARACTERISTICS (ABRIDGED)

JQ353 B52 – Primary Characteristics		
Voltage Sensitivity	mV/g	500
Frequency Range (±5%)	Hz	0.1 to 2000
Frequency Range (±5° phase)	Hz	0.2 to 2000
Noise – Broadband	g rms	160e-6
Weight	oz	1.1
Measurement Range	±g pk	10
Spectral Noise: (1 Hz)	g / sqrt(Hz)	200 e-6
(10 Hz)	g / sqrt(Hz)	16 e-6
(100 Hz)	g / sqrt(Hz)	5 e-6

393 M52 – Primary Characteristics		
Voltage Sensitivity	mV/g	1000
Frequency Range (±5%)	Hz	0.125 to 2000
Frequency Range (±5°)	Hz	0.75 to 2000
Noise – Broadband	g rms	17.4e-6
Weight	oz	7.4
Measurement Range	±g pk	5
Spectral Noise: (1 Hz)	g / sqrt(Hz)	1 e-6
(10 Hz)	g / sqrt(Hz)	0.2 e-6
(100 Hz)	g / sqrt(Hz)	0.1 e-6

352 M12 – Primary Characteristics		
Voltage Sensitivity	mV/g	1000
Frequency Range (±5%)	Hz	0.2 to 4000
Frequency Range (±5° phase)	Hz	0.4 to 4000
Noise – Broadband	g rms	59e-6
Weight	oz	1.3
Measurement Range	±g pk	2
Spectral Noise: (1 Hz)	g / sqrt(Hz)	5e-6
(10 Hz)	g / sqrt(Hz)	2e-6
(100 Hz)	g / sqrt(Hz)	1e-6

370 A02 – Primary Characteristics		
Voltage Sensitivity	mV/g	100
Frequency Range (±5%)	Hz	0 to 300
Frequency Range (±5° phase)	Hz	0 to 50
Noise – Broadband	g rms	0.0007
Weight	oz	0.39
Measurement Range	±g pk	15
Spectral Noise: (1 Hz)	g / sqrt(Hz)	150 e-6
(10 Hz)	g / sqrt(Hz)	45 e-6
(100 Hz)	g / sqrt(Hz)	15 e-6

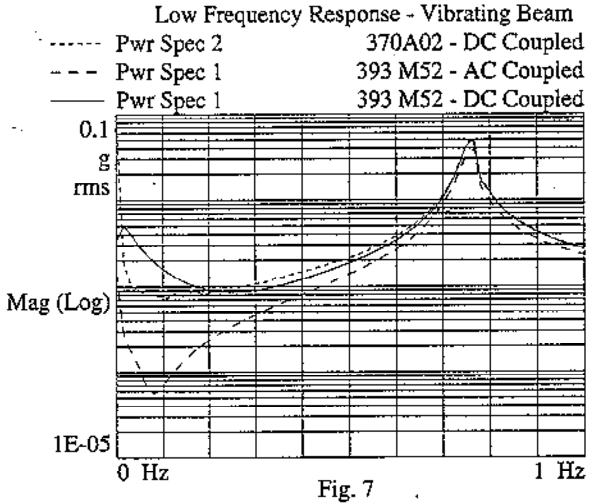

Fig. 7

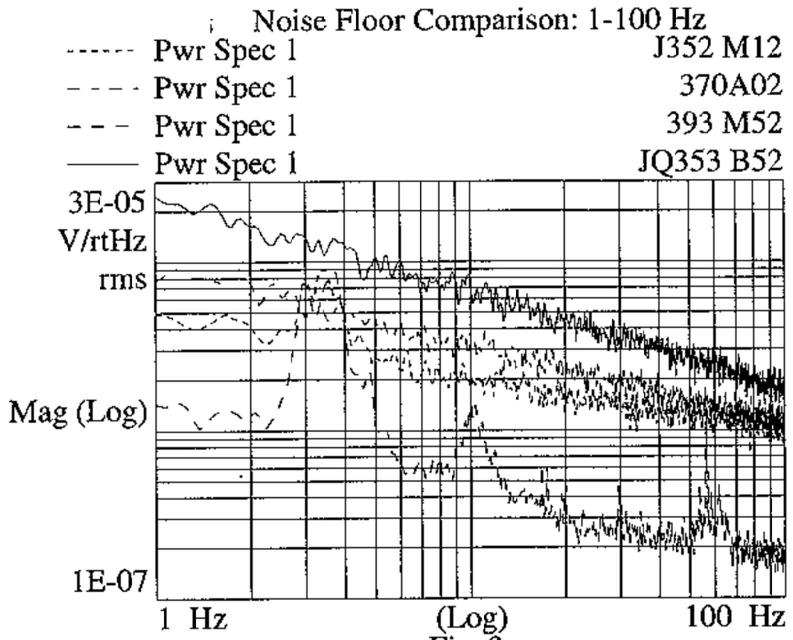

Fig. 3.

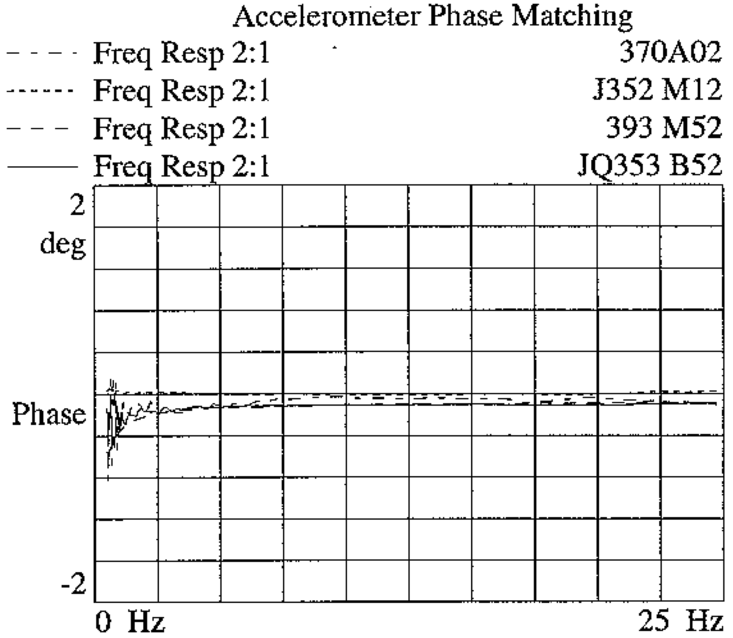

Fig. 4.

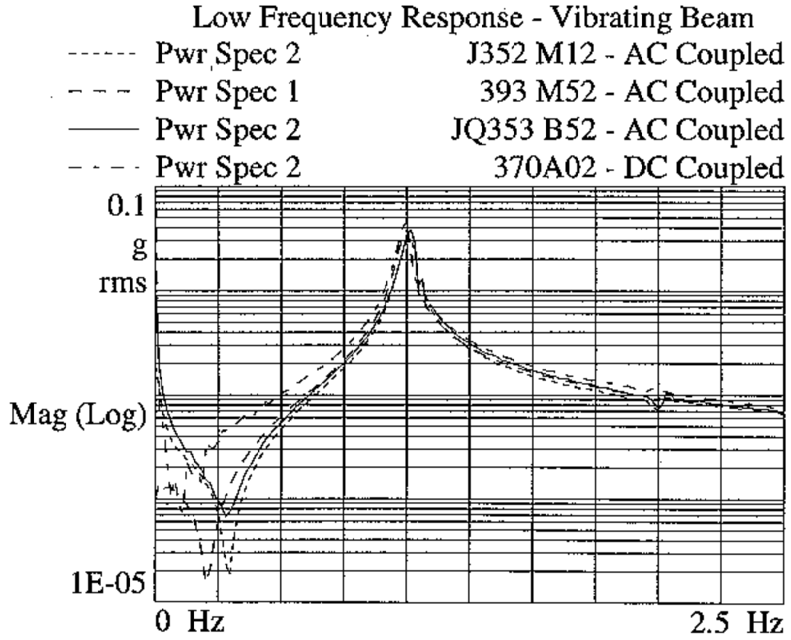

Fig. 5.

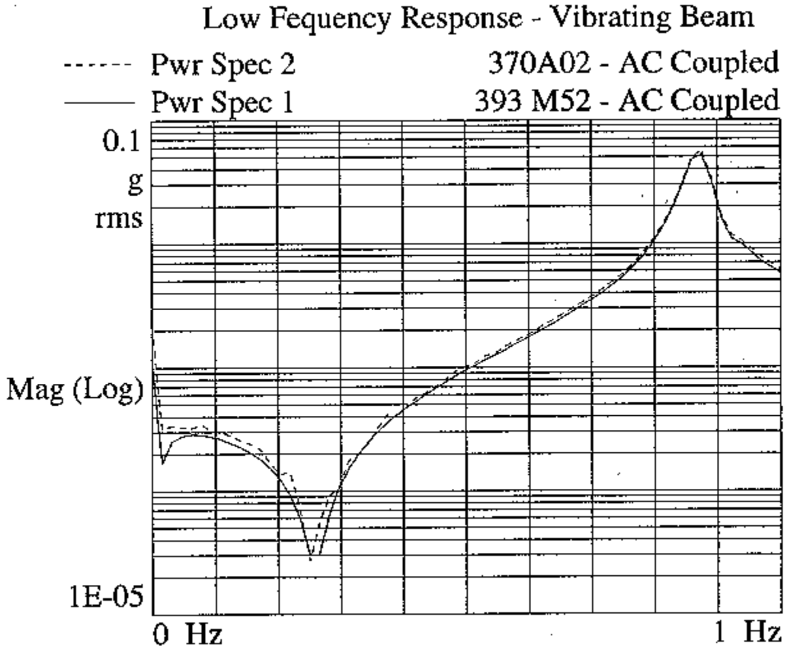

Fig. 6.